HHS Public Access

Author manuscript

Acta Biomater. Author manuscript; available in PMC 2020 July 01.

Published in final edited form as:

Acta Biomater. 2019 July 01; 92: 71–81. doi:10.1016/j.actbio.2019.05.019.

Zwitterionic poly-carboxybetaine coating reduces artificial lung thrombosis in sheep and rabbits

Rei Ukita, **Neil M. Carleton**, **Noritsugu Naito**, **Angela Lai**, **Chi Chi Do-Nguyen**, **Caitlin T. Demarest**, and **Keith E. Cook**

Department of Biomedical Engineering, Carnegie Mellon University, 5000 Forbes Avenue, Scott Hall 4th Floor, Pittsburgh PA 15213

Kan Wu, **Xiaojie Lin**, and **Shaoyi Jiang**

Department of Chemical Engineering, University of Washington, Box 351750, Seattle, Washington 98195-1750, USA

Abstract

Current artificial lungs fail in 1–4 weeks due to surface-induced thrombosis. Biomaterial coatings may be applied to anticoagulate artificial surfaces, but none have shown marked long-term effectiveness. Poly-carboxybetaine (pCB) coatings have shown promising results in reducing protein and platelet-fouling *in vitro*. However, *in vivo* hemocompatibility remains to be investigated. Thus, three different pCB-grafting approaches to artificial lung surfaces were first investigated: 1) graft-to approach using 3,4-dihydroxyphenylalanine (DOPA) conjugated with pCB (DOPA-pCB); 2) graft-from approach using the Activators ReGenerated by Electron Transfer method of atom transfer radical polymerization (ARGET-ATRP); and 3) graft-to approach using pCB randomly copolymerized with hydrophobic moieties. One device coated with each of these methods and one uncoated device were attached in parallel within a veno-venous sheep extracorporeal circuit with no continuous anticoagulation (N=5 circuits). The DOPA-pCB approach showed the least increase in blood flow resistance and the lowest incidence of device failure over 36-hours. Next, we further investigated the impact of tip-to-tip DOPA-pCB coating in a 4-hour rabbit study with veno-venous micro-artificial lung circuit at a higher activated clotting time of 220–300s (N≥5). Here, DOPA-pCB reduced fibrin formation ($p=0.06$) and gross thrombus formation by 59% ($p<0.05$). Therefore, DOPA-pCB is a promising material for improving the anticoagulation of artificial lungs.

Graphical Abstract

Corresponding Author Information: Name: Rei Ukita, rei.ukita@vumc.org.
Present Address: Vanderbilt University Medical Center, Department of Thoracic Surgery, 609 Oxford House, 1313 21st Avenue South, Nashville TN 37232, Phone Number: 832-344-7012, FAX Number: 615-936-7003

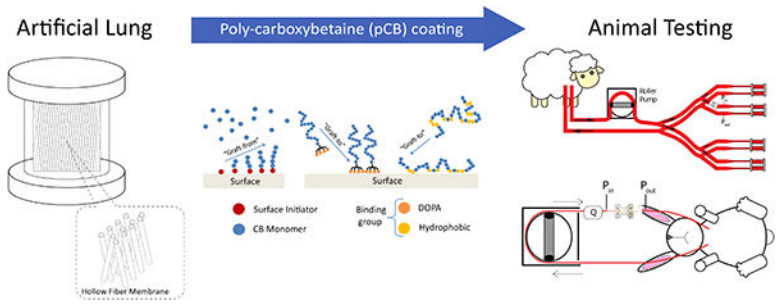

Keywords

artificial lung; thrombosis; zwitterion; carboxybetaine; 3,4-dihydroxyphenylalanine (DOPA)

1. Introduction

Over 168,000 Americans die every year due to chronic respiratory diseases [1–4]. The only long-term treatment option is lung transplantation, but only 2,345 lung transplants take place each year in the United States [5]. Extracorporeal membrane oxygenation (ECMO) is an alternative means of long-term respiratory support which performs gas exchange using a densely-packed bed of hydrophobic hollow fibers. However, these fiber surfaces are especially susceptible to surface-induced coagulation, ultimately resulting in device failure within 1–4 weeks [6–8]. Currently, heparin is intravenously administered as an anticoagulant to prolong the device lifespan, but bleeding complications are prevalent and often fatal during ECMO [9,10]. Hence, an alternative anticoagulation approach with minimal systemic effect would be highly desirable.

To reduce thrombosis only at blood-contacting surfaces, anticoagulant molecules such as heparin and low-fouling polymers such as polyethylene glycol (PEG) have been applied over oxygenator surfaces. However, the existing coating technology is not sufficient for extending the device's useful lifetime. Surface-bound heparin has reduced bioactivity compared to its soluble form [11], and several studies have reported no clear benefits of PEG coatings when in contact with whole blood [12–14].

Carboxybetaine (CB), on the other hand, is a newer class of low-fouling molecule that has shown promising *in vitro* results for repelling protein and platelet fouling [15–18]. CB is zwitterionic, defined as having both positive and negative charges while retaining a net neutral charge. The equal and opposite charges present on zwitterionic molecule electrostatically attract water molecules, forming a robust hydration layer that repels non-specific protein adsorption [19]. Previous work has coated hydrophobic surfaces such as poly-(dimethyl siloxane) (PDMS) and polypropylene (PP) with poly-carboxybetaine (pCB) chains using graft-from approach via ARGET-ATRP [16] (Figure 1a), as well as graft-to approaches via DOPA [16],[17],[20] (Figure 1b) and random copolymerization of CB and hydrophobic monomers (Figure 1c). These coated surfaces repelled non-specific protein adsorption and platelet adhesion efficiently even in complex media, including 100% plasma [18]. Although pCB has shown excellent *in vitro* performances in multiple studies,[15–

18,20] several challenges exist for extending this to artificial lung applications. First, artificial lungs' gas exchange membrane surfaces are densely packed and complex in surface geometry. Additionally, an artificial lung circuit has multiple distinct types of synthetic polymer, which also raises the difficulty of achieving a uniform grafting across different surface characteristics. Finally, artificial lungs must repel non-specific protein adsorption under a rigorous, whole blood environment. Therefore, an ideal coating methodology specifically for artificial lungs must be determined, and its ability to impede clot formation must be evaluated in a clinically relevant model.

In the following studies, the optimal method of attaching pCB to the artificial lung surfaces was evaluated with two separate *in vivo* experiments. In the first, oxygenators with different pCB coating methods were attached in parallel in a 36-hour, sheep, veno-venous ECMO model. To achieve measurable clotting within the 36-hour time frame, sheep were not continuously anticoagulated. Under this rigorous whole blood environment with no anticoagulation, three different pCB attachment methods were compared. In each case, the goal was to develop a simple, flow-through coating method that would not significantly complicate the artificial lung construction process. The first coating used the graft-to method, in which direct surface attachment of pCB polymer chains was accomplished using the previously reported DOPA-pCB conjugate [20]. The second adsorbed pCB to surfaces after copolymerizing it with a hydrophobic moiety. Lastly, the third utilized a "graft-from" approach using ARGET-ATRP. In the following *in vivo* study, the coating that exhibited the best performance in the sheep studies was further investigated to determine its ability to slow clot formation when used alone and with the entire circuit coated using the same method. This second study utilized a four-hour rabbit veno-venous extracorporeal circuit model with continuous anticoagulation to better reflect the clinical environment. Both studies will serve as a necessary, intermediate investigation of pCB coating *in vivo* prior to the ultimate, long-term evaluation in a full-scale artificial lung.

2. Experimental Section

The animal housing and surgical procedures were approved by the Allegheny-Singer Research Institute's Institutional Animal Care and Use Committee in accordance with institution and federal regulations.

2.1. Sheep Study

2.1.1. Sheep Study, Miniature Artificial Lung Fabrication—Microporous PP hollow fiber membrane (outer diameter = 200 μm, Type X30–150, 3M,NC) was coated with thin poly-siloxane layer (Applied Membrane Technology, MN). The siloxane-PP fiber was double-layered and knitted with a crossing angle of 30 degrees and fiber spacing of 43 fibers/inch. The mat was rolled into a fiber bundle with a path length of 1.5 cm. The bundle was then encapsulated in a PETG housing (McMaster-Carr, IL) and "potted" in place using PDMS (Elastosil RT 625, Wacker Chemie AG, Germany). Polyurethane filling (WC-575, BJB Enterprises, CA) was injected into the corner areas of the device at the cap-housing interface to reduce areas of stagnation and recirculation. Silicone tubing with inner diameter (ID) of 3/16" (McMaster-Carr, IL) was attached as blood inlet and outlet for the device. For

this work, the devices did not have gas inlet or outlet because the focus was primarily on thrombosis initiated at blood-material interface. The completed device (Figure 2a) had a total fiber surface area of 0.1 m^2 and a frontal area of 14.5 cm^2. After fabrication, the device was coated with one of the three methodologies described below.

2.1.2. pCB Coating—CB monomers were synthesized according to a previously reported method [21]. *n*-Butyl methacrylate (BMA) and 2-trimethylammoniumethyl methacrylate chloride (TMAEMA) were purchased from Tokyo Chemical Industry Co., Ltd. (OR). 3-[Tris(trimethylsiloxy)silyl]propyl methacrylate (MTS) was obtained from Sigma-Aldrich (MO).

i. DOPA-pCB: DOPA-pCB conjugate was synthesized using a method similar to one described previously [20], but carboxybetaine methacrylate (CBMA) was used as the monomer instead of CBAA. This DOPA-pCB conjugate was then mixed in a water-methanol solution (80%/20% v/v) to achieve a concentration of 2 mg/mL, and 2-amino-2-hydroxymethyl-propane-1,3-diol (TRIS) salt was added to reach a pH of 8.5. The sample was incubated with this solution and then agitated for 20 hours. ii) Random Copolymer: CB random copolymers, poly(CBAA-*co*-BMA) and poly(CBAA-*co*-MTS-*co*-TMAEMA) were synthesized by conventional free radical polymerization method using AIBN as an initiator, in a method similar to that reported previously [22–24]. In brief, the desired amounts of monomer and AIBN were dissolved into ethanol. The solution was further bubbled with nitrogen gas for 30 minutes at room temperature. Polymerization was performed in the sealed glass tube under a protection atmosphere of nitrogen gas. After that, the polymer was purified by precipitation. The coating copolymers were dissolved in ethanol-water (8:2 volume-volume ratio), each at a 1% weight ratio. Samples were soaked with this solution for 1 hour, emptied, and dried overnight. This process was repeated two more times.

ii. ARGET-ATRP pCB: The miniature artificial lung was completed filled with hydrogen peroxide/18.4 M sulfuric acid solution (30%/70% v/v) and then exposed for 60 seconds to hydroxylate the surfaces. Subsequently, the ARGET methodology followed our previously reported methodology [16].

iii. Surface characterization: Coated fiber surfaces on miniature artificial lungs were characterized using X-ray photoemission spectroscopy (XPS). Nitrogen atoms only exist in the pCB polymer chains but not in PP or PDMS that make up the base substrate, so nitrogen intensity in survey scan was used to prove the presence of pCB coating. All tested samples were taken from the outmost layer of fiber bundles and cut in to 1 cm x 1 cm squares. Without any treatment, all samples were subject to a monochromatized Electron Spectroscopy for Chemical Analysis (ESCA) system (Kratos AXIS Ultra DLD, Manchester, UK) under high vacuum.

iv. Quality Control: Each batch of CB polymer underwent a quality control step using smaller pieces of PDMS-PP hollow fiber membrane. The same PDMS-PP

fiber mat used for artificial lung fabrication was heat-sealed and cut into small rectangular pieces, each with dimensions of 0.25” x 0.5” such that the shorter edge is perpendicular to the hollow fibers. This fiber piece was coated with the batch of CB polymer and tested for fibrinogen-fouling via enzyme-linked immunosorbent assay (ELISA), as described previously [16,17,20]. Only the batch that reduced fibrinogen fouling by at least 90% compared to the uncoated control was used to coat artificial lungs.

2.1.3. Sheep Study, Circuit Preparation—The miniature artificial lung was attached in a veno-venous, extracorporeal, parallel circuit configuration (Figure 2b). The 18–28 French dual lumen cannula (Avalon Elite, Maquet, NJ) provided both drainage and reinfusion. Tygon tubing was used for the circuit tubing material. The drainage cannula was followed by 220 cm of 3/8” ID tubing (Cole-Parmer, IL), followed by 75 cm of ¼” ID tubing (Saint-Gobain, France), which then fed into the portion of the circuit containing four artificial lungs in-parallel. Before entering the parallel lungs, blood flow from the cannula was divided into four separate branches using a 1/4”- 1/4” polycarbonate Y connector (Qosina, NY), followed by 10 cm of 1/4” ID tubing, and then another 1/4”-1/4” polycarbonate Y connector. After the second Y connector, each branch contained, in order: 6.5 cm of ID 1/4” tubing; 1/4”-3/16” polycarbonate reducer (Qosina, NY); 5 cm of ID 3/16” tubing (Saint-Gobain, Courbevoie, France); 3/16”-3/16” polycarbonate luer connector (Qosina, NY); miniature artificial lung; 3/16”-3/16” polycarbonate luer connector; 5 cm of ID 3/16” tubing; 1/4”-3/16” polycarbonate reducer; 6.5 cm of ID 1/4” tubing. Four separate branches converged back to one flow using the same set of Y connectors as before for diverging the flow, but in a reverse order. Finally, 200 cm of 1/4” ID tubing, followed by 40 cm of 3/8” ID tubing, were used to direct the flow back to dual lumen cannula for reinfusion.

2.1.4. Sheep Study, Surgery—Two Montadale sheep were used for this study. Transdermal fentanyl patches (Apotext Corp, FL, 75 μg/hr) were applied to the sheep 12 hours before the surgery, and anesthesia was induced via intravenous injection of 4–6 mg/kg propofol (Fresenius Kabi, Germany). During the surgery, the sheep’s native lungs were ventilated with an inhalational anesthetic of 1–5 % isoflurane in pure oxygen. A beveled pressure tubing (TruWave, Edwards Lifesciences, CA) was placed as arterial line in the carotid artery to obtain blood samples and mean arterial pressure (MAP) measurements. The dual lumen ECMO cannula was placed via the jugular vein and tunneled to the right atrium for drainage and reinfusion for the extracorporeal circuit. At initial attachment, the circuit was primed with saline containing 5000 units of heparin (Sagent, IL) and 30 mg/kg of methylprednisolone sodium succinate (Pfizer, NY). The initial attachment circuit did not include artificial lungs. Instead, the first device attachment was offset by at least 6 hours after the surgery, following the attachment protocol (see *Attachment and Detachment*).

The roller pump (COBE, CO) was used to achieve a total blood flow rate of 800 mL/min through the cannula and 200 ± 20 mL/min per branch. After the attachment surgery, the sheep was moved to a custom-built stanchion cage. Once the sheep was awake and alert

post-surgery, it was transported to the animal facility for chronic monitoring and artificial lung attachment.

2.1.5. Sheep Study, Artificial Lung Attachment and Detachment—The first set of attachment was performed at least 6 hours after the surgery. Moreover, the devices were primed with normal saline at least 6 hours before the attachment to ensure that surfaces were sufficiently wetted. Prior to attachment, sheep was given an IV bolus of 50 units heparin/kg. The devices were attached two at a time using the following protocol. First, the total blood flow was reduced from 800 to 400 mL/min. Next, the circuit was clamped off after the first Y connector and right before the last Y connector to cut off blood flow from half of the circuit. The clamped-off section was removed and replaced with a primed device circuit containing two artificial lungs. The clamps were removed, and the flow was returned to 800 mL/min and adjusted further by placing adjustable clamps on each branch to ensure even distribution between the four branches. Once the flow through each device was at 200 ± 20 mL/min, initial baseline resistance measurement was recorded. After the baseline measurements were taken for both devices, the same set of procedure was followed for initial attachment of other two branches/devices.

Each artificial lung was detached from the main circuit 36 hours after attachment or when it met the failure criteria defined as follows: two consecutive resistance measurements were 100% greater than the initial, baseline resistance value. Prior to detachment, sheep were given an intravenous bolus of heparin (50 units/kg). The total blood flow was reduced to 200 mL/min per remaining device prior to device removal. After detachment, a piece of 3/16” ID Tygon tubing was put in the place of the removed lung. To keep the flow equal between all four branches, a Hoffman clamp was placed distal to each device outlet and adjusted accordingly. Each removed circuit was rinsed with a bolus of heparin (10,000 units) followed by heparinized saline (2 units/mL) until the effluent became colorless. Afterwards, the device was fixed with 2% glutaraldehyde (Electron Microscopy Sciences, PA) in phosphate buffer.

After all the devices from the first set were removed, a new set of devices was re-attached up to two more times afterwards if platelet count was at least 2/3rds of the baseline value. All devices were primed with saline for at least 6 hours prior to attachment to ensure that the surfaces were hydrated. Prior to re-attachment, sheep were given a bolus of 50 units/kg of heparin. After a maximum of 3 sets of devices, each sheep was given 0.22 mL/kg of sodium pentobarbital (Vortech Pharmaceuticals Ltd, MI) intravenously for euthanasia.

2.1.6. Sheep Management—During monitoring, the sheep was given either an intravenous drip of either saline or Lactated Ringer’s solution at 1.2–5 mL/kg/hr. There was no continuous administration of anticoagulants in order to accelerate coagulation for this experiment. The fentanyl dermal patch was started 12 hours prior to the surgery and maintained for 72 hours. After the patch wore off, the sheep was given an intramuscular injection of 0.005–0.01 mg/kg buprenorphine every 4–8 hours (Renckitt Benckiser Pharmaceuticals, England). For antibiotics, 5 mg/kg enrofloxacin (Bayer, Germany) was given intravenously once a day, and 40,000 units/kg of procaine penicillin G/benzathine penicillin G combination (Aspen Veterinary Resources, MO) was given intramuscularly

every 72 hours. The animal's arterial blood samples were taken to measure activated clotting time (ACT), hematocrit, and arterial blood gas (ABG) as needed or every 6 hours. Platelet and white blood cell counts were taken twice a day and plasma-free hemoglobin once a day.

2.1.7. Sheep Study, Digital Data—Mean arterial pressure was measured with patient monitor (Tram-rac 4A with Tram 600SL module, GE Marquette Electronics, WI). Device inlet and outlet pressures for each coating type were measured using Transpac transducers (ICU Medical Inc, CA). Flow rate was monitored using ultrasonic flow probe and flow meter (TS410 with 14PXL, NY). Both sets of measurements were recorded onto the monitoring computer using data acquisition system (Biopac Systems, CA). Blood flow resistance was calculated as: (inlet pressure – outlet pressure)/device flow rate.

2.1.8. Sheep Study, Data Processing and Statistical Analysis—The resistance measurements were log-transformed. For all statistical tests with repeated measures, a mixed linear model was used with animal subject and/or device number as the subject variables, time as the repeated measure, coating and time as fixed effects, and Autoregressive(1) as the repeated covariance matrix. Bonferroni correction was used for post-hoc correction for all pairwise comparisons. For devices that failed before the 36-hour time limit, the last recorded resistance measurement was kept until the 36-hour mark as a conservative estimate of the resistance had it been left attached. The Kaplan-Meier method was performed to compare device failure rates, using log rank as the statistical test for significant difference in failure rate. A p-value < 0.05 was considered statistical significance for all tests. The error bars in the figures represent standard error of the mean (S.E.M.) unless stated otherwise.

2.2. Rabbit Study

2.2.1. Rabbit Study, Micro Artificial Lung Fabrication—The same PDMS-PP fiber from the sheep study was used for these devices. The double-layered hollow fiber mat was heat-sealed and cut into 0.85" x 0.85" squares. Ten of these squares were layered in the same orientation and melted on all four sides to create a single fiber pack, until its lateral dimensions were 0.615" x 0.615". Seven of the fiber packs were fitted into 1.34"-long square polycarbonate tube (ID = 0.625", Part # 3161T21, McMaster-Carr, IL) for a total fiber surface area of 400 cm^2. Custom-made polycarbonate square caps were fitted onto both ends of the tube and sealed with silicone RTV (McMaster-Carr, IL). The other end of the square cap was fitted with thread-to-barbed adapters (Qosina, NY). The completed device is shown in Figure 2c.

2.2.2. Rabbit Study, Circuit Preparation—The micro artificial lung was attached in a veno-venous extracorporeal circuit configuration (Figure 2d). The device inlet circuit components consisted of: 7 cm of 60-cm-pressure tubing with four side-holes serving as inflow cannula; male luer with spin lock-to-barb connector (Qosina, NY); 75 cm of 3/16" ID tubing; 3/16"–1/4" polycarbonate reducer; 9 cm of 1/4" ID tubing; 3/16"–1/4" polycarbonate reducer; 5 cm of 3/16" ID tubing; 3/16"–3/16" polycarbonate Luer connector (NovoSci, TX); 5 cm of 3/16" ID tubing. The device outlet circuit components are: 5 cm of 3/16" ID tubing; 3/16"–3/16" polycarbonate Luer connector; 25 cm of 3/16" ID tubing; and a 14-gauge angiocatheter (Becton Dickinson, NJ) as the outflow cannula. The circuit was

coated tip-to-tip with DOPA-pCB for the coating group using the previously described methodology. The uncoated group had the same circuit components without the coating. On the day of the experiment, the circuit was primed with saline and 10 mg/kg of sodium methylprednisolone.

2.2.3. Animal Management—New Zealand white rabbits (Average weight = 3.6 +/− 0.4 kg) were initially sedated with subcutaneous injection of 30 mg/kg of ketamine (Vedco Inc, MO) and 5 mg/kg of xylazine (Akorn Animal Health, IL). They were then intubated and attached to the ventilator using 100% O_2 with 1–5% isoflurane for anesthesia during the experiment. An intravenous drip of Lactated Ringer's solution was also started at 10–30 mL/kg/hr.

A 16-gauge angiocatheter (Becton Dickinson, NJ) was placed in the carotid artery for both blood sampling, MAP measurements, and drug delivery. A continuous intravenous drip of phenylephrine was then started using a syringe pump (New Era Pump Systems Inc, NY) at a rate between 0.5 and 5 μg/kg/min in order to maintain normal blood pressure. All baseline blood samples and measurements were taken at this point (see 2.2.4. Blood Sampling). For circuit attachment, a 16-gauge angiocatheter was first inserted into the left internal jugular vein as the reinfusion site. Heparin infusion was then started at the left jugular incision site at 1 unit/min to prevent clot formation. For drainage cannula, a pressure tubing (VLMF120, Edwards Lifesciences, CA) was cut to a length of 6 cm with a bevel in a direction opposite of cannula's curvature to prevent suctioning against vessel wall. Three side-holes were cut out near the beveled tip, and this cannula was inserted into the right internal jugular vein as the drainage cannula until its tip reached the right atrium. Blood flow through the circuit was maintained at 45 mL/min with a roller pump (COBE, CO). Heparin infusion rate was kept between 60 and 120 units/hour to maintain ACT between 220 and 300 seconds.

2.2.4. Blood Sampling—Rabbit arterial blood was drawn for determining the activated clotting time (ACT), arterial blood gas (ABG), platelet counts, and enzyme-linked immunosorbent assays (ELISA) for pselectin and fibrinopeptide A. These blood samples were all taken at baseline, and 10, 30, 120, and 240 minutes after circuit attachment. Additionally, ACT was also taken at 60 and 180 minutes. Heparinized syringes were used for ELISA samples. For platelet counts, syringes were citrated at 9:1 v/v ratio blood:ACD (Santa Cruz Biotechnology, CA). Arterial blood gas measurement was taken using heparinized syringe.

The activated clotting time was measured using a Hemochron Response Whole Blood Coagulation System (Accriva Diagnostics, San Diego, CA). Arterial blood gas (ABG) was measured with ABL Flex 800 gas analyzer (Radiometer, Copenhagen, Denmark) for monitoring health and measuring hemoglobin level; and platelet counts were taken with a Z1 Dual Threshold Coulter Counter (Beckman Coulter, Brea, CA) following the manufacturer's specifications for platelets. For the ELISAs, 2 mL of whole blood was collected in a heparinized syringe and then centrifuged at 1000g for 20 minutes. The plasma supernatant was collected and immediately frozen at −20 °C. ELISA kits (MyBioSource, San Diego, CA) were used for rabbit soluble p-selectin (Catalog #: MBS011457) and rabbit

fibrinopeptide A (Catalog #: MBS013487). The instruction manuals were followed for measuring plasma level of each protein.

2.2.5. Rabbit Study, Digital Data—The same procedure was followed from that of chronic sheep study to measure blood pressures, flow rate, and resistance.

2.2.6. Device Detachment and Autopsy—Four hours after the circuit attachment, rabbits were given 10,000 units of heparin intravenously in preparation for circuit detachment. The entire circuit was then detached and flushed with saline until the effluent became clear. After circuit removal, rabbits were euthanized with 2 mEq/kg of intravenous potassium (Hospira, IL). The micro artificial lung was then removed from the rest of the circuit and dried with a gentle stream of air until no moisture could be detected.

The device was weighed, and the change in device weight between the beginning and end of the experiment was recorded as the clot weight. The micro artificial lung was then fixed in 2% glutaraldehyde solution in 0.2 M phosphate buffer for scanning electron microscopy. Hollow fiber pieces were excised from the center of the fiber layer at the inlet, middle, and outlet of the bundle. These samples were dehydrated with 25, 50, 75, and 100% ethanol solutions in water. Fiber samples were then sputter coated with platinum at 3 nm thickness. The images were taken with 5 kV accelerating voltage, spot size of 3.0, and magnification levels between 50 and 2000 (Philips XL-30, Netherlands).

2.2.7. Data Processing and Statistical Analysis—Prior to statistical analysis, platelet count and clotting factor levels were first corrected for hemodilution caused by circuit attachment, and normalized to baseline, pre-attachment, as follows: corrected data = raw data × HemoglobinbBaseline/Hemoglobint=10 min (Supplementary Information Fig. S2: Hemoglobin data). A mixed linear model was used to analyze clotting factor levels, ACT, log(resistance), and platelet count in the same fashion as the sheep study. The device clot weight was compared using Student's t-test. The clotting factor levels and platelet count were represented as the change from its baseline value.

3. Results

3.1. Surface characterization

The presence of pCB coating layer on the fiber bundles was confirmed by characterizing the surface atomic composition using XPS (Figure 3, Table S1). Across all four surface types, the XPS survey scan detected peaks from carbon (C 1s), oxygen (O 1s), and silicon (Si 1s) which make up the outer layer of PDMS-PP hollow fibers. From the same scan, nitrogen (N 1s) could not be detected on uncoated surface, whereas there were significant N 1s peaks for random copolymer surface at atomic percentage of 2.72%, DOPA-pCB at 2.26%, and ARGET-ATRP at 2.71% (Figure 3a, Table S1). There were also concomitant decreases in silicon percentages from 21.73% for the uncoated surface down to 10.65% for random copolymer, 6.66% for ARGETATRP, and 14.85% for DOPA-pCB.

The detailed C 1s, N 1s and O 1s signatures were further studied, as shown in the representative high resolution spectra for DOPA-pCB (Figure 3b). The C 1s signals were

fitted with Gaussian model into four components based on their respective binding energies, including carbon bonds from C-C (284.8 eV), $-N^{+}(CH_3)_2$- (285.9 eV), carboxyl (287.9 eV), and amide (289.6 eV). Similarly, the O 1s signals were assigned to three peaks: oxygen bonds of Si-O (530.2 eV), C=O (531.5 eV), and C-O (533.0 eV). The N 1s were assigned into two peaks: nitrogen bonds of amide bond (399.9 eV), and quaternary amine (402.2 eV), both of which correspond to the nitrogen atom on the CB moieties. Based on spectral analyses, both atomic and bond profiles of the surface strongly suggest that pCB chains were successfully grafted onto hollow fiber surfaces.

3.2. Sheep Study

Five sets of devices were tested in two different sheep. Three sets of devices were attached to the first sheep and two sets to the second. One DOPA-pCB device from the first sheep was removed early at a 12-hour mark due to a high resistance measurement. However, this device showed low amount of clot formation that did not match up with its recorded resistance, and it was found later that the same pressure transducer was malfunctioning. Hence, this DOPA-pCB device was removed from subsequent analysis, leaving N = 4 for DOPA-pCB. The entire second set from the second sheep was also terminated early at a 34-hour mark due to early euthanasia. The average ACT across all time points for both sheep was 152 ± 30 s (mean ± standard deviation). The log(resistance) (mmHg/(L/min)) across all time points for each surface type is shown in Figure 4a. The DOPA-pCB coated devices had the lowest resistance and the smallest deviation between sets. The copolymer coating showed a significantly higher log(resistance) than DOPA-pCB, ARGETATRP, and uncoated ($p < 0.01$, < 0.05, and < 0.05, respectively). The other pairwise comparisons did not show any significant difference (Table S2). The failure curve from these same sets of devices is shown in Figure 4b. DOPA-pCB had the lowest failure rate of 25%, followed by ARGET-ATRP (40%), uncoated (60%), and copolymer (80%). The copolymer devices failed at a significantly higher rate than DOPA-pCB devices ($p < 0.05$). Due to the small sample size and large variabilities, however, no significant differences in failure rate were seen between uncoated and DOPA-pCB ($p = 0.24$) or between rest of the other pairings ($p = 0.1117 – 0.574$). Whereas more sheep experiments could have been performed to achieve statistical significance, we decided to instead proceed with the rabbit experiment to conduct a study that focuses on one type of coating under a more clinically relevant setting. For this following study, DOPA-pCB coating was selected as it showed the lowest rate of failure.

3.3. Rabbit Study

Initially, seven rabbits were used for the uncoated control group, and six rabbits for the DOPA-pCB group. However, 1 rabbit in the uncoated control group and 1 rabbit in the DOPA-pCB group were completely discarded because the ACT did not fit the proposed range. Two rabbits' platelet count data, one from each group, were also discarded because both cases showed an abnormally low platelet count at baseline ($<1\times10^8$ cells/mL) that increased to more than 1.5×10^8 cells/mL at the 10-minute mark, leaving N = 4 for DOPA-pCB and N = 5 for uncoated.

The ACTs were not significantly different between the two groups over the 4-hour period (Supplementary Information Figure S3, uncoated = 241 ± 43 s, DOPA-pCB = 260 ± 44 s,

mean ± SD, p = 0.21). The average baseline platelet count (x 10^8 platelets/mL, mean ± SD) for uncoated and DOPA-pCB was 1.60 ± 0.20 and 1.76 ± 0.24, respectively (N = 4 and 5, respectively). The change in device weight was significantly different between groups ($p < 0.05$, Figure 5a). The coating group had 59% less clot weight than the uncoated after the 4-hour study. The clot formation throughout the study was recorded by measuring device's blood flow resistance (Figure 5b). Both groups showed a common trend, in which there was an initial spike in the first 2 hours, but the value dropped back down and stabilized for the remainder of the experiment (Figure 5b). The uncoated control's resistance was consistently higher in magnitude than DOPA-pCB, but there was no significant difference between the groups due to the large variation between rabbits (p = 0.18). The scanning electron microscopy images showed that the DOPA-pCB coating reduced microscopic clot formation on both the hollow gas exchange fibers (Figure 6, top) as well as the finer weaving fibers (Figure 6, bottom). These results indicate that the gross clot formation was reduced with DOPA-pCB tip-to-tip coating.

To better understand how DOPA-pCB reduced thrombus formation, blood coagulation and platelet activation were studied with ELISAs and platelet counts. The level of plasma fibrinopeptide A (FPA), produced as a byproduct from fibrin generation, is shown in Figure 7 as a change from the baseline. For both groups, there was an increase within 30 minutes after attachment, but this spike was suppressed in the coated case. The peak occurred after 10 minutes for uncoated and 30 minutes for the DOPA-pCB, but the average FPA level was consistently higher in the uncoated case. The overall difference approached statistical significance between groups (p = 0.06). The platelet count (Figure 8a) decreased significantly over time for both groups ($p < 0.05$) but showed no significant difference between groups (p = 0.45). Additionally, the soluble pselectin level, which is released by activated platelets, showed no statistically significant differences between groups (Figure 8b). These data suggest that DOPA-pCB coating has a substantial effect on reducing the coagulation cascade activity; however, there was no measurable effect on systemic platelet activation in this experimental setting.

4. Discussion

This study was conducted to evaluate *in vivo* efficacy of pCB coatings in two steps. First, each grafting methodology was carried out over miniature artificial lung surfaces, and the coated lungs were tested in a parallel veno-venous circuit for a fair assessment of coatings. The anticoagulant function of the most promising method was then studied independently in a four-hour rabbit veno-venous model with a clinically relevant ACT. Although the devices used in the sheep study are smaller than those used in clinical ECMO, the 0.1 m^2 surface area and the packed bed geometry of the fiber bundle still pose a challenge for achieving a uniform surface coverage. Furthermore, the miniature artificial lung in the study consists of multiple of materials: PDMS potting, tubing, and hollow fibers; polypropylene weaving fibers; PETG housing; and polyurethane filling. Achieving an effective coating over various surface compositions and geometries using one fixed coating process is challenging.

The surface elemental analysis with XPS demonstrated the presence of nitrogen atoms characteristic to CB moieties for all three coating methods inside miniature lungs.

Furthermore, the percentage of nitrogen atoms matched closely with the value of 2.4% reported by the study by Amoako et al, which coated a 7.7 cm^2 flat PDMS sheet with DOPA-pCB.[18] The coatings in the present study not only achieved high grafting efficiency that was comparable to its previous work, but they were also achieved over larger, more complex surfaces. The high-resolution spectral analysis further demonstrated that the chemical bonds on the surface corresponded to those of CB moieties.

These three coatings and the uncoated control were tested head-to-head in a parallel venovenous sheep circuit. Out of the four types of surfaces tested, the copolymer coating showed the quickest increase in resistance with an overall failure rate of 80%. The ARGET coating had only a slightly lower failure rate than the uncoated. The DOPA-pCB coating not only had the lowest failure rate of 25%, but also had the most consistent results within the group. DOPA is a versatile adhesive molecule that can stably attach to a variety of surfaces through different possible mechanisms [20,25,26]. Hence, it may be that DOPA-pCB was the most effective in part because there are multiple surface materials like artificial lungs. The ARGET-ATRP graft-from methodology can theoretically achieve a higher grafting density by covalently attaching initiator molecules to the surface and then polymerizing CB monomers. However, ARGET-ATRP is costlier and attaching initiators is challenging. In the current study, a piranha solution was used to graft the initiators, serving as a powerful oxidizing agent to hydroxylate organic surfaces. In addition to its safety risks, the reagent also raises a concern about material degradation that may lead to premature device failure. Regardless, ARGET-ATRP devices had highly variable resistance values between sets and exhibited a similar failure trend as the uncoated in this study (Figure 4). This may also be due to the challenges of scaling up the ARGET-ATRP methodology to larger, more complex surfaces compared to smaller, simpler surfaces tested in previous studies [16]. Finally, the random copolymerization approach has been used for physiosorption of highly hydrophilic zwitterionic polymers to hydrophobic surfaces [23,27]. This method is the most established and often utilized for commercial coatings, but its effectiveness may depend on the substrate surface. However, this approach led to faster increase in resistance compared to the uncoated control in this study. Potentially, the exposed hydrophobic blocks accelerated the clotting process. Two types of hydrophobic copolymers were used in this study: methyl trisiloxane for PDMS coating and butyl methacrylate for PP weaving fiber coating. Further optimization of each of these polymers may lead to improved future performance.

In the second set of the second sheep, however, the copolymer device showed no marked increase in resistance for the entire duration. The first four copolymer devices were primed in saline for about 6 hours, whereas the fifth one was primed for over 72 hours while waiting for sheep platelet numbers to increase. This longer wetting time may have contributed to that copolymer coating's improved blood biocompatibility. The 6- to 12-hour period may not be long enough for fully hydrating an artificial lung such that the hydrophobic residues were still largely exposed to the blood-side and hence promoted protein adsorption. Chen *et al* reported that the length of wetting time of PP substrate coated with zwitterionic phosphorylcholine or sulfobetaine copolymer affected the contact angle (i.e. hydrophilicity), and that there was a dramatic drop-off in contact angle within the first few minutes [28]. This previous study, however, evaluated this change in hydrophilicity over small, flat surface. In the current study, a fiber bundle consists of 43 double-layers of packed beds of

hollow fibers with a total surface area of 0.1 m^2. Any portion of the bundle that was not sufficiently wetted would likely contribute to premature failure. This critical length of time required for fiber bundle wetting may be the underlying reason for early failure in copolymer coatings, and this aspect needs to be investigated and improved for future copolymer coating applications in artificial lungs.

Overall, the sheep study showed that the DOPA methodology may be the most effective method for attaching pCB chains to artificial lung surfaces. Moreover, the sheep model evaluated pCB-coating efficacy over a large, complex surface under rigorous whole blood environment, which has never been demonstrated before. However, this alone does not provide enough information about the effects of coating. Because of the parallel configuration of the extracorporeal circuit, the benefits of one successful coating on the coagulation system may be confounded and obscured by the presence of other less successful ones, the control device, and the uncoated circuit. The polycarbonate connectors present throughout the circuit are especially prone to thrombus formation because they introduce geometrical steps in the circuit, so their presence puts even more of a challenge for the coatings. Moreover, these lungs were miniature devices without fully optimized fluid mechanics. Finally, there was no continuous administration of heparin anticoagulation to sheep, and sheep were only given heparin boluses intermittently. The rationale for this experimental design was to accelerate clotting and observe measurable changes within the 36-hour time frame. Otherwise, the duration would have to be extended to at least one week for clinical oxygenators to actually fail [6–8]. At an ACT of 152 ± 30 s (mean ± standard deviation) across all time points between two sheep, the surfaces were subjected to highly procoagulant bloodstream than clinical ECMO standard, which recommends ACT between 180 and 220 seconds [29]. The pCB coatings in this study can only repel non-specific adsorption but have no means of inhibiting activated platelets or coagulation factors. Thus, coatings will have limited benefit when the remainder of the circuit, particularly the circuit inlet, are rapidly producing thrombus. In a similar study using ECMO without anticoagulation, Lai *et al.* found a precipitous increase in failure rate at around 36 hours, even in devices with relatively slower clot formation [30].

The follow-up rabbit study was thus designed to examine the devices under a more clinically relevant setting. Only one type of coating was tested per animal to focus on each surface type's effect on the coagulation system. Furthermore, the entire circuit was coated tip-to-tip to minimize the confounding effects of uncoated surfaces, and the rabbit was also given a continuous drip of heparin to keep ACT between 220 and 300 seconds. Hence, the experimental design of the rabbit study better reflects how the coatings will be used in future clinical applications.

In the rabbit study, the macroscopic clot formation was significantly reduced with DOPA-pCB coating as demonstrated by the significant reduction of device clot weight (Figure 5a). Furthermore, the electron microscope images also confirm that micron-scale clot formation was suppressed over both hollow and weaving fiber surfaces (Figure 6). Finer weaving fibers tend to generate denser clots compared to the hollow fibers and can be especially challenging to coat [31]. These 10 μm-diameter fiber strands are tightly wound together, so the interstices form stagnant regions that can easily entrap platelets and accumulate

procoagulant factors, making them challenging areas for reducing fouling. The SEM images from this study suggest that the DOPA-pCB coating was grafted successfully even to the fine weaving fibers and reduced coagulation over these areas as well.

The other supporting data suggest that the DOPA-pCB coating reduced clot formation by reducing the contact activation of coagulation cascade. The coating's effect becomes apparent in the first 60 minutes, as seen in the FPA level and the device resistance. The most marked increase in FPA occurs in the first 10 minutes for the uncoated case, but this was mitigated with DOPA-pCB coating. The large surge in FPA level can be attributed to the initial exposure of blood to artificial material which elicits the most extreme response from the intrinsic pathway. With the low-fouling coating, the contact activation of the intrinsic pathway was reduced, so the rate of FPA generation decreased. The rapid increase in resistance also occurred within the first hour for the uncoated but substantially less in the DOPA-pCB group. The contact activation led to rapid formation of thrombus within the uncoated device, occlusion of the blood flow, and consequently the marked increase in resistance. Because the peak in resistance occurred at different time points between devices, this led to large variability between devices, so the difference approached, but did not achieve, significance.

The FPA and resistance data showed a similar trajectory over the 4-hour period: a rapid increase, followed by a slight drop, and finally a plateau. The contact activation in the initial stage leads to acceleration of the coagulation process, resulting in the rapid rise in fibrin formation and thus FPA level and device resistance. After the initial spike, clot formation slows, presumably due to exhaustion of procoagulant zymogens and activation of the fibrinolytic system. While clot is forming, fibrin also catalyzes fibrinolysis by increasing the rate of conversion of inactive plasminogen to plasmin [32], and enhancing clot breakdown in the micro-lung. The end-result in this early experimental phase is a shift from rapid coagulation toward clot dissolution.

Whereas the coatings clearly reduced coagulation, there was no significant effect of DOPA-pCB coating on the p-selectin expression or the platelet count. This trend may be caused by the peristaltic pump, which has been shown to cause shear-induced activation and micro-aggregation of platelets [33,34]. Hence, the coating's benefit on platelet function and preservation may be outweighed by the shear-induced activation from the pump. The platelet data here, however, appears to contradict some of the previous studies investigating zwitterionic coatings' effects on platelets, including those conducted by Amoako *et al* [18] and Wang *et al* [35]. It is important to point out several key differences between these studies and the present study, which likely caused this discrepancy. Amoako *et al* showed that DOPA-pCB reduced platelet adhesion on a PDMS membrane *in vitro*, but they did not investigate systemic platelet count [18]. On the other hand, Wang *et al* demonstrated in a canine study that the systemic platelet count was better preserved when the PP hollow fiber oxygenator was coated with cross-linkable phosphorylcholine[35]. However, Wang *et al*'s canine study, as well as Amoako *et al*'s study, deviated in the anticoagulation approach from the clinical ECMO practice because citrate was used instead of heparin. Citrate is a platelet inhibitor through calcium chelation. Unlike that study, the rabbit studies in this paper followed the clinical ECMO standard and used heparin as anticoagulant. Heparin provides

no platelet inhibition other than reducing thrombin formation and can even directly activate platelets and lead to a reduction in platelet count in a small number of patients.[36,37] Thus pCB coatings may not affect platelet counts when heparin anticoagulation is used with a pump, as during clinical ECMO. Their ability to inhibit clot formation, therefore, is likely due to inhibition of the intrinsic branch of the coagulation cascade.

This study was a rigorous *in vivo* evaluation of pCB coating over artificial lung surfaces at a clinical or lower level of anticoagulation. This was a large step-up in complexity and challenge for pCB coating compared to previous studies [17,18,38]. It is common for coatings to be effective in single-protein solutions or plasma, but to be inadequate when tested *in vivo* against whole blood [12–14]. Previous studies have also been done on smaller, simpler surfaces [17,18,20,38], which does not scale up to a larger surface or translate to more complex geometry such as a fiber bundle in this presented work. Despite these additional obstacles, DOPA-pCB coating reduced thrombus formation in an artificial lung. Success in this study suggests that further studies examining DOPA-pCB coatings during long-term, weeks-long ECMO at clinically relevant ACTs should be pursued. At the same time, the results also suggest that coating alone may not completely inhibit thrombosis. There may be areas inside the artificial lung circuit that did not achieve high enough of a grafting density, so these parts may be more prone to clot formation. Additionally, there are other contributors to thrombosis, such as shear-induced activation by the pump, and recirculation and stagnation in areas like device inlet and outlet where blood flow patterns rapidly change. Combining pCB with an additional, surface-focused anticoagulation approach may overcome this limitation. For instance, functionalizing the carboxylate groups in pCB with anticoagulant drugs or proteins may further reduce surface-coagulation [39,40]. Another promising approach is to inhibit Factor XII activity in the intrinsic coagulation pathway to specifically reduce surface-induced thrombosis [41,42]. Thus, future studies will combine pCB coating with these approaches to further cut down on surface-induced thrombosis in artificial lungs [43,44]. With surface-focused anticoagulation, tip-to-tip pCB coating, and optimized device design for blood flow through the device, a better coating performance would be expected to achieve a longer device lifetime than the clinical oxygenators. If successful in that setting, this synergistic, surface-focused approach would be able to reduce thrombotic and bleeding complications. Ultimately, this could reduce patient mortality as well.

Supplementary Material

Refer to Web version on PubMed Central for supplementary material.

Acknowledgments

The authors acknowledge the funding source for this research: 2R01HL089043. The authors also acknowledge use of the Materials Characterization Facility at Carnegie Mellon University supported by grant MCF-677785 for the scanning electron microscopy images.

References

[1]. Murphy SL, Xu J, Kochanek KD, Curtin SC, Arias E, Deaths: Final data for 2015, Natl. Vital Stat. Reports 66 (2017). doi:10.1136/vr.h753.

[2]. Cystic Fibrosis Foundation Patient Registry 2016 Annual Data Report, Bethesda, Maryland, 2017.

[3]. Olson AL, Swigris JJ, Lezotte DC, Norris JM, Wilson CG, Brown KK, Mortality from Pulmonary Fibrosis Increased in the United States from 1992 to 2003, Am. J. Respir. Crit. Care Med. 176 (2007) 277–284. doi:10.1164/rccm.200701-044OC. [PubMed: 17478620]

[4]. Hutchinson JP, McKeever TM, Fogarty AW, Navaratnam V, Hubbard RB, Increasing global mortality from idiopathic pulmonary fibrosis in the twenty-first century., Ann. Am. Thorac. Soc 11 (2014) 1176–1185. doi:10.1513/AnnalsATS.201404-145OC. [PubMed: 25165873]

[5]. Valapour M, Lehr CJ, Skeans MA, Smith JM, Carrico R, Uccellini K, Lehman R, Robinson A, Israni AK, Snyder JJ, Kasiske BL, OPTN/SRTR 2016 Annual Data Report: Lung, Am. J. Transplant 18 (2018) 363–433. doi:10.1111/ajt.14562. [PubMed: 29292602]

[6]. Fischer S, Simon AR, Welte T, Hoeper MM, Meyer A, Tessmann R, Gohrbandt B, Gottlieb J, Haverich A, Strueber M, Bridge to lung transplantation with the novel pumpless interventional lung assist device NovaLung, J. Thorac. Cardiovasc. Surg 131 (2006) 719–723. doi:10.1016/j.jtcvs.2005.10.050. [PubMed: 16515929]

[7]. Haneya A, Philipp A, Mueller T, Lubnow M, Pfeifer M, Zink W, Hilker M, Schmid C, Hirt S, Extracorporeal Circulatory Systems as a Bridge to Lung Transplantation at Remote Transplant Centers, Ann. Thorac. Surg 91 (2011) 250–255. doi:10.1016/j.athoracsur.2010.09.005. [PubMed: 21172523]

[8]. Maul TM, ECMO Anticoagulation: It's Still the Biggest Challenge!, in: ASAIO 61st Annu. Conf., Chicago, 2015.

[9]. Dalton HJ, Garcia-Filion P, Holubkov R, Moler FW, Shanley T, Heidemann S, Meert K, Berg RA, Berger J, Carcillo J, Newth C, Harrison R, Doctor A, Rycus P, Dean JM, Jenkins T, Nicholson C, Association of bleeding and thrombosis with outcome in Extracorporeal Life Support, Pediatr. Crit. Care Med. 16 (2015) 167–174. doi:10.1097/PCC.0000000000000317. [PubMed: 25647124]

[10]. Mazzeffi M, Greenwood J, Tanaka K, Menaker J, Rector R, Herr D, Kon Z, Lee J, Griffith B, Rajagopal K, Pham S, Bleeding, Transfusion, and Mortality on Extracorporeal Life Support: ECLS Working Group on Thrombosis and Hemostasis, Ann. Thorac. Surg 101 (2016) 682–689. doi:10.1016/j.athoracsur.2015.07.046. [PubMed: 26443879]

[11]. Gorman RC, Ziats NP, Rao AK, Gikakis N, Sun L, Khan MMH, Stenach N, Sapatnekar S, Chouhan V, Gorman JH, Niewiarowski S, Colman RW, Anderson JM, Edmunds LH, Surface-bound heparin fails to reduce thrombin formation during clinical cardiopulmonary bypass, J. Thorac. Cardiovasc. Surg 111 (1996) 1–12. doi:10.1016/S0022-5223(96)70395-1. [PubMed: 8551753]

[12]. Park K, Shim HS, Dewanjee MK, Eigler NL, In vitro and in vivo studies of PEO-grafted blood-contacting cardiovascular prostheses, J. Biomater. Sci. Polym. Ed 11 (2000) 1121–1134. doi:10.1163/156856200744228. [PubMed: 11263803]

[13]. Kidane A, Lantz GC, Jo S, Park K, Surface modification with PEO-containing triblock copolymer for improved biocompatibility: In vitro and ex vivo studies, J. Biomater. Sci. Polym. Ed 10 (1999) 1089–1105. doi:10.1163/156856299X00702. [PubMed: 10591134]

[14]. Shen M, Martinson L, Wagner MS, Castner DG, Ratner BD, Horbett TA, PEO-like plasma polymerized tetraglyme surface interactions with leukocytes and proteins: In vitro and in vivo studies, J. Biomater. Sci. Polym. Ed 13 (2002) 367–390. doi:10.1163/156856202320253910. [PubMed: 12160299]

[15]. Ladd J, Zhang Z, Chen S, Hower JC, Jiang S, Zwitterionic polymers exhibiting high resistance to nonspecific protein adsorption from human serum and plasma, Biomacromolecules. 9 (2008) 1357–1361. doi:10.1021/bm701301s. [PubMed: 18376858]

[16]. Hong D, Hung HC, Wu K, Lin X, Sun F, Zhang P, Liu S, Cook KE, Jiang S, Achieving Ultralow Fouling under Ambient Conditions via Surface-Initiated ARGET ATRP of Carboxybetaine, ACS Appl. Mater. Interfaces 9 (2017) 9255–9259.doi:10.1021/acsami.7b01530. [PubMed: 28252277]

[17]. Sundaram HS, Han X, Nowinski AK, Brault ND, Li Y, Ella-Menye J-R, Amoaka K. a., Cook KE, Marek P, Senecal K, Jiang S, Achieving One-Step Surface Coating of Highly Hydrophilic Poly(Carboxybetaine Methacrylate) Polymers on Hydrophobic and Hydrophilic Surfaces, Adv. Mater. Interfaces 1 (2014) n/a–n/a. doi:10.1002/admi.201400071.

[18]. Amoako KA, Sundaram HS, Suhaib A, Jiang S, Cook KE, Multimodal, Biomaterial-Focused Anticoagulation via Superlow Fouling Zwitterionic Functional Groups Coupled with Anti-Platelet Nitric Oxide Release, Adv. Mater. Interfaces 3 (2016) 1–9. doi:10.1002/admi.201500646.

[19]. Jiang SY, Cao ZQ, Ultralow-fouling, functionalizable, and hydrolyzable zwitterionic materials and their derivatives for biological applications, Adv. Mater 22 (2010) 920–932. [PubMed: 20217815]

[20]. Sun F, Wu K, Hung HC, Zhang P, Che X, Smith J, Lin X, Li B, Jain P, Yu Q, Jiang S, Paper Sensor Coated with a Poly(carboxybetaine)-Multiple DOPA Conjugate via Dip-Coating for Biosensing in Complex Media, Anal. Chem 89 (2017) 10999–11004. doi:10.1021/acs.analchem.7b02876. [PubMed: 28921971]

[21]. Zhang Z, Vaisocherová H, Cheng G, Yang W, Xue H, Jiang S, Nonfouling Behavior of Polycarboxybetaine-Grafted Surfaces: Structural and Environmental Effects, Biomacromolecules. 9 (2008) 2686–2692. doi:10.1021/bm800407r. [PubMed: 18785772]

[22]. Lin X, Konno T, Ishihara K, Cell-Membrane-Permeable and Cytocompatible Phospholipid Polymer Nanoprobes Conjugated with Molecular Beacons, Biomacromolecules. 15 (2014) 150–157. doi:10.1021/bm401430k. [PubMed: 24308501]

[23]. Lin X, Fukazawa K, Ishihara K, Photoreactive Polymers Bearing a Zwitterionic Phosphorylcholine Group for Surface Modification of Biomaterials, ACS Appl. Mater. Interfaces 7 (2015) 17489–17498. doi:10.1021/acsami.5b05193. [PubMed: 26202385]

[24]. Lin X, Fukazawa K, Ishihara K, Photoinduced inhibition of DNA unwinding in vitro with water-soluble polymers containing both phosphorylcholine and photoreactive groups., Acta Biomater. 40 (2016) 226–234. doi:10.1016/j.actbio.2016.03.040. [PubMed: 27045692]

[25]. Kord Forooshani P, Lee BP, Recent approaches in designing bioadhesive materials inspired by mussel adhesive protein, J. Polym. Sci. A. Polym. Chem 55 (2017) 9–33. doi:10.1002/pola.28368. [PubMed: 27917020]

[26]. Lee H, Scherer NF, Messersmith PB, Single-molecule mechanics of mussel adhesion, Proc. Natl. Acad. Sci 103 (2006) 12999 LP-13003. http://www.pnas.org/content/103/35/12999.abstract. [PubMed: 16920796]

[27]. Ishihara K, Bioinspired phospholipid polymer biomaterials for making high performance artificial organs, Sci. Technol. Adv. Mater 1 (2000) 131–138. doi:10.1016/S1468-6996(00)00012-7.

[28]. Chen SH, Chang Y, Ishihara K, Reduced blood cell adhesion on polypropylene substrates through a simple surface zwitterionization, Langmuir. 33 (2017) 611–621. doi:10.1021/acs.langmuir.6b03295. [PubMed: 27802598]

[29]. Laurance L, Annich G, Al-Ibrahim M, Bembea Omar, Brodie D, Brogan T, Buckvold S, Chicoine L, Conrad S, Cooper D, Dalton H, Frischer J, Harris B, Mazor R, Paden M, Rintoul N, Ryerson L, Spinella P, Teruya J, Winkler A, Wong T, Massicotte MP., ELSO Anticoagulation Guideline, Ann Arbor, MI, 2014 https://www.elso.org/portals/0/files/elsoanticoagulationguideline8-2014-table-contents.pdf.

[30]. Lai A, Do-Nguyen CC, Demarest CT, Ukita R, Skoog DJ, Carleton NM, Amoako KA, Montoya PJ, Cook KE, Short Term in vivo Evaluation of Nitric Oxide Generating Artificial Lung in Sheep, in: ASAIO 63rd Annu. Conf. Abstr., Chiago, 2017: p. 112.

[31]. Ye S-H, Arazawa DT, Zhu Y, Shankarraman V, Malkin AD, Kimmel JD, Gamble LJ, Ishihara K, Federspiel WJ, Wagner WR, Hollow Fiber Membrane Modification with Functional Zwitterionic Macromolecules for Improved Thromboresistance in Artificial Lungs, Langmuir. (2015) 10.1021/la504907m.

[32]. Thorsen S, The Mechanism of Plasminogen Activation and the Variability of the Fibrin Effector during Tissue- type Plasminogen Activator—mediated Fibrinolysis, Ann. N. Y. Acad. Sci 667 (1992) 52–63. doi:10.1111/j.1749-6632.1992.tb51597.x. [PubMed: 1309072]

[33]. Borgdorff P, Fekkes D, Tangelder GJ, Hypotension Caused by Extracorporeal Circulation, Circulation. 106 (2002) 2588 LP-2593. http://circ.ahajournals.org/content/106/20/2588.abstract. [PubMed: 12427656]

[34]. Linneweber J, Chow TW, Kawamura M, Moake JL, Nosè Y, In Vitro Comparison of Blood Pump Induced Platelet Microaggregates between a Centrifugal and Roller Pump During

Cardiopulmonary Bypass, Int. J. Artif. Organs 25 (2002) 549–555. doi: 10.1177/039139880202500610. [PubMed: 12117295]

[35]. Wang YB, Shi KH, Jiang HL, Gong YK, Significantly reduced adsorption and activation of blood components in a membrane oxygenator system coated with crosslinkable zwitterionic copolymer, Acta Biomater. 40 (2016) 153–161.doi:10.1016/j.actbio.2016.02.036. [PubMed: 26969525]

[36]. Saba HI, Saba SR, Morelli GA, Effect of heparin on platelet aggregation., Am. J. Hematol 17 (1984) 295–306. [PubMed: 6475940]

[37]. Xiao Z, Theroux P, Platelet activation with unfractionated heparin at therapeutic concentrations and comparisons with a low-molecular-weight heparin and with a direct thrombin inhibitor., Circulation. 97 (1998) 251–256. [PubMed: 9462526]

[38]. Yang W, Bai T, Carr LR, Keefe AJ, Xu J, Xue H, Irvin C. a., Chen S, Wang J, Jiang S, The effect of lightly crosslinked poly(carboxybetaine) hydrogel coating on the performance of sensors in whole blood, Biomaterials. 33 (2012) 7945–7951. doi:10.1016/j.biomaterials.2012.07.035. [PubMed: 22863377]

[39]. Jiang S, Cao Z, Ultralow-fouling, functionalizable, and hydrolyzable zwitterionic materials and their derivatives for biological applications, Adv. Mater 22 (2010) 920–932. doi:10.1002/adma. 200901407. [PubMed: 20217815]

[40]. Vaisocherová H, Yang W, Zhang Z, Cao Z, Cheng G, Piliarik M, Homola J, Jiang S, Ultralow Fouling and Functionalizable Surface Chemistry Based on a Zwitterionic Polymer Enabling Sensitive and Specific Protein Detection in Undiluted Blood Plasma, Anal. Chem 80 (2008) 7894–7901. doi:10.1021/ac8015888. [PubMed: 18808152]

[41]. Baeriswyl V, Calzavarini S, Chen S, Zorzi A, Bologna L, Angelillo-Scherrer A, Heinis C, A Synthetic Factor XIIa Inhibitor Blocks Selectively Intrinsic Coagulation Initiation, ACS Chem. Biol 10 (2015) 1861–1870. doi:10.1021/acschembio.5b00103. [PubMed: 25989088]

[42]. Middendorp SJ, Wilbs J, Quarroz C, Calzavarini S, Angelillo-Scherrer A, Heinis C, Peptide Macrocycle Inhibitor of Coagulation Factor XII with Subnanomolar Affinity and High Target Selectivity, J. Med. Chem 60 (2017) 1151–1158.doi:10.1021/acs.jmedchem.6b01548. [PubMed: 28045547]

[43]. Cooke AR, Demarest CT, Wilbs J, Heinis C, Cook KE, Targeted FXII Inhibition for Localized Anticoagulation Effects in Artificial Lungs, in: ASAIO 63rd Annu. Conf., Chicago, 2017: p. 114.

[44]. Naito N, Ukita R, Carleton NM, Bouloubassis K, Cook KE, Combined Use of a Selective Factor XII Inhibitor with a Polycarboxybetaine Surface Coating Generates Potent Artificial Lung Anticoagulation Without Bleeding., in: Soc. Thorac. Surg. 55th Annu. Meet., San Diego, CA, 2019.

Statement of significance

Chronic lung diseases lead to 168,000 deaths each year in America, but only 2,300 lung transplantations happen each year. Hollow fiber membrane oxygenators are clinically used as artificial lungs to provide respiratory support for patients, but their long-term viability is hindered by surface-induced clot formation that leads to premature device failure. Among different coatings investigated for blood-contacting applications, poly-carboxybetaine (pCB) coatings have shown remarkable reduction in protein adsorption *in vitro*. However, their efficacy *in vivo* remains unclear. This is the first work that investigates various pCB-coating methods on artificial lung surfaces and their biocompatibility in sheep and rabbit studies. This work highlights the promise of applying pCB coatings on artificial lungs to extend its durability and enable long-term respiratory support for lung disease patients.

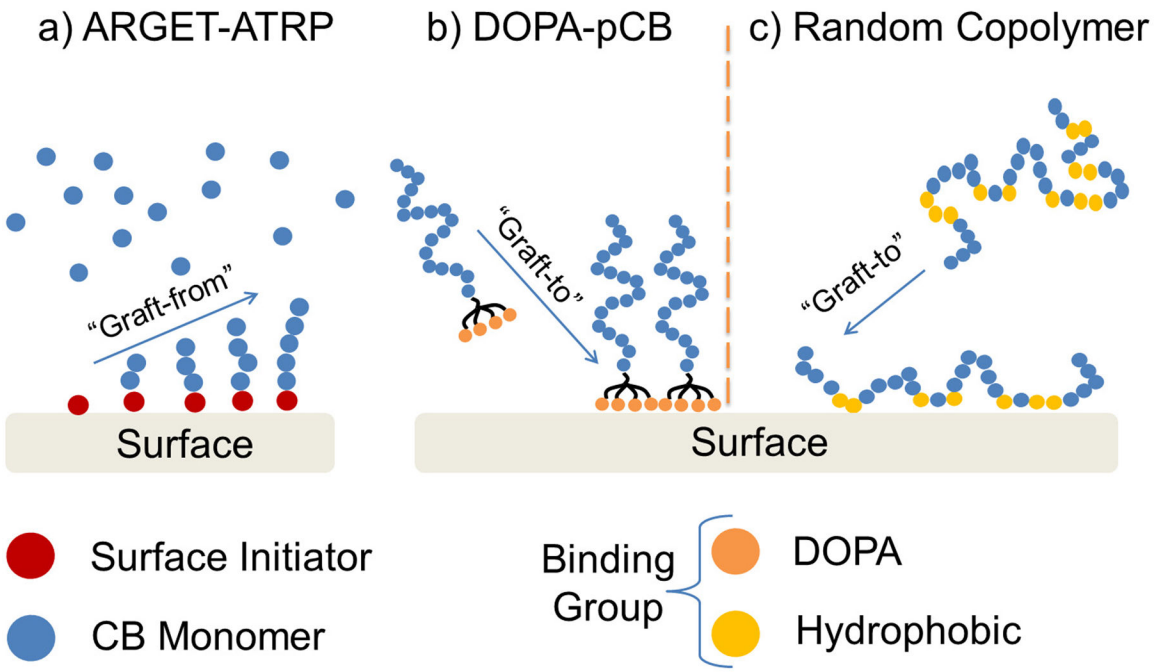

Figure 1:
Schematics illustrating different grafting techniques for pCB, such as graft-from approach using a) ARGET-ATRP, and graft-to approaches using b) DOPA molecules and c) random copolymerization of CB and hydrophobic monomers. Chemical structures are shown in Figure S1 in Supplementary Information.

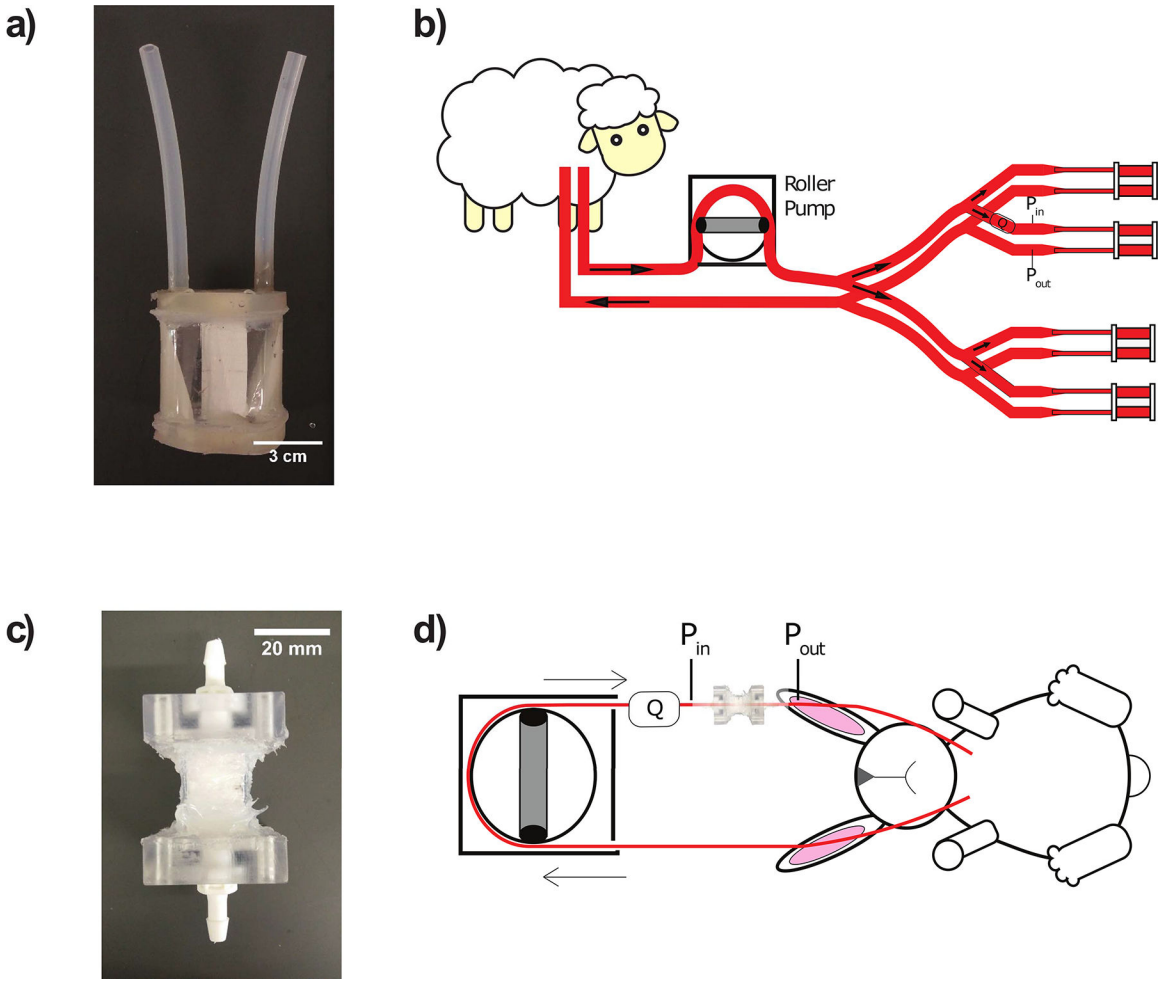

Figure 2:

Fabricated artificial lungs and animal extracorporeal circuit diagrams: a) miniature artificial lung (fiber surface area = 0.1 m^2); b) sheep veno-venous parallel extracorporeal circuit featuring miniature artificial lungs coated with one of four methods (uncoated control, graft-to DOPA-pCB, graft-from ARGET-ATRP, graft-to copolymer). Each device's thromboresistance is tracked by measuring flow rate (Q) with flow probe and pressure drop ($P_{in} - P_{out}$) with pressure transducers to calculate resistance; c) micro artificial lung used for rabbit study (fiber surface area = 400 cm^2); d) rabbit veno-venous extracorporeal circuit, with or without tip-to-tip pCB coating

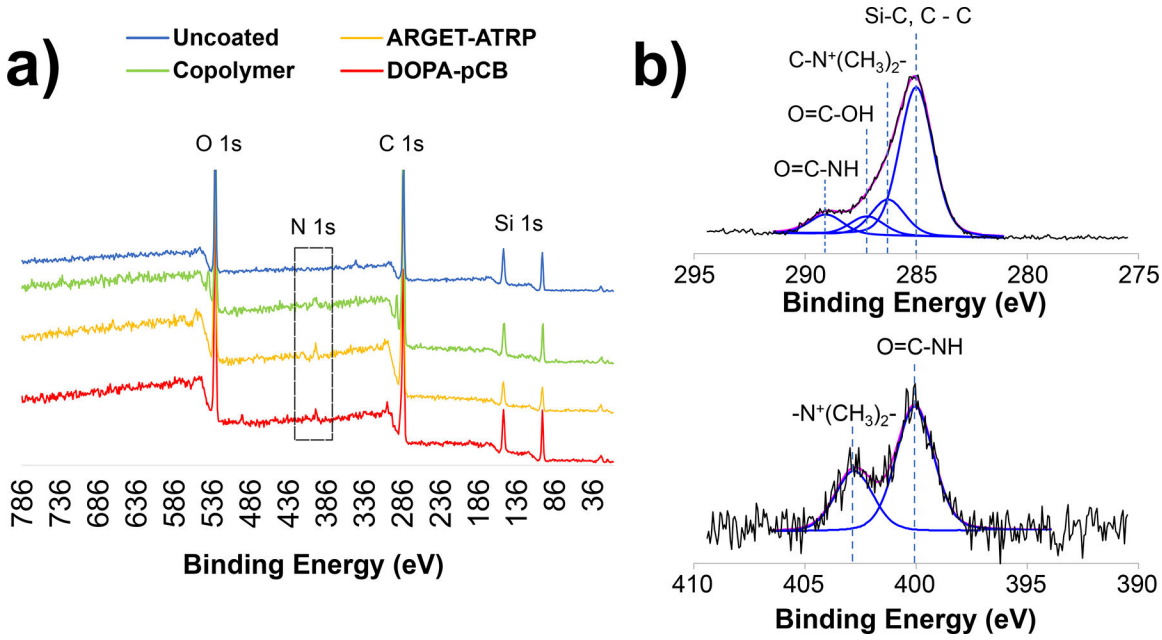

Figure 3:

X-ray photoemission spectroscopy analysis of coated fiber surfaces in miniature artificial lung: a) survey scan of uncoated and pCB-coated surfaces; the dotted box shows that nitrogen was present on the three coated surfaces but not on the uncoated surface; b) high-resolution scan of DOPA-pCB surface shows the types of carbon bonds (top) and nitrogen (bottom) that correspond to CB moieties

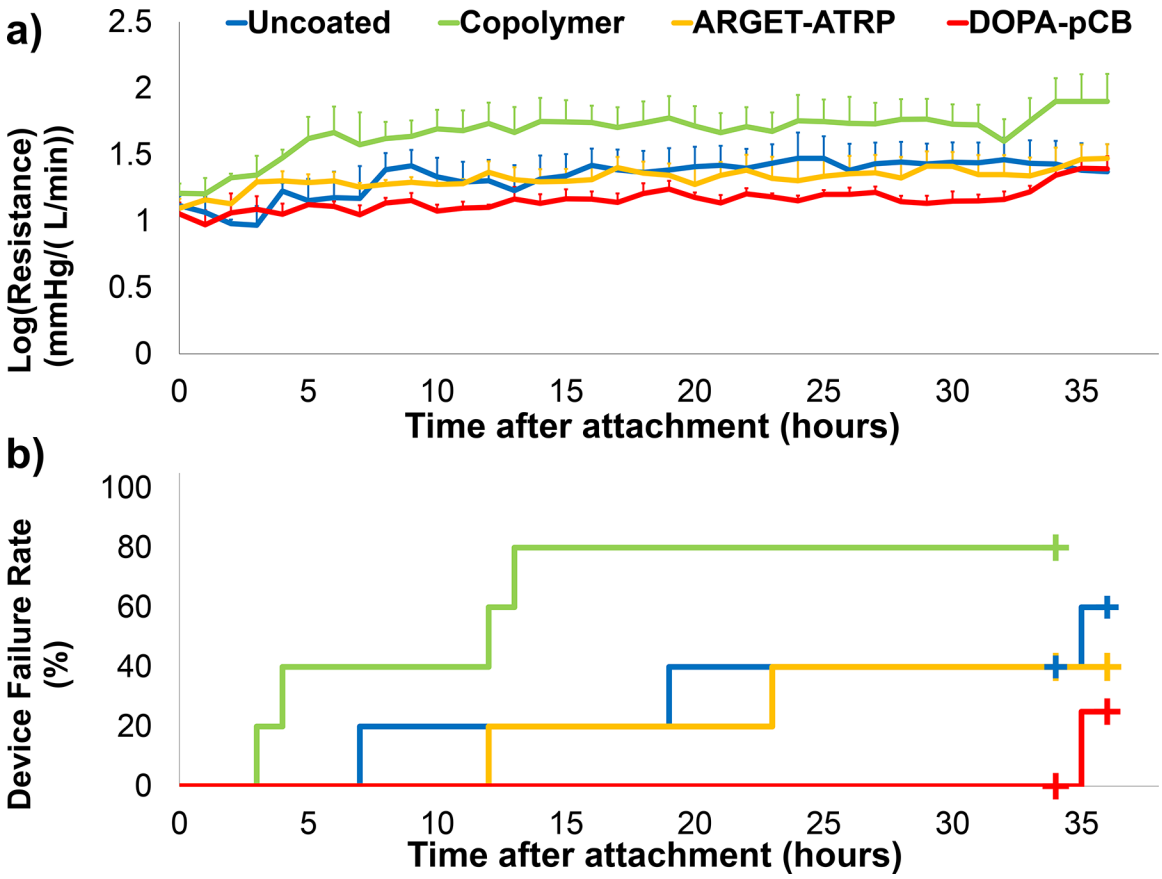

Figure 4:

a) Device log(resistance) for each coating type over the 36-hour period (N = 5 for uncoated, ARGET-ATRP, Copolymer; N = 4 for DOPA-pCB; error bars = S.E.M. b) Device failure curve plotted over the 36-hour period for the same set of devices; plus signs (+) indicate censored events.

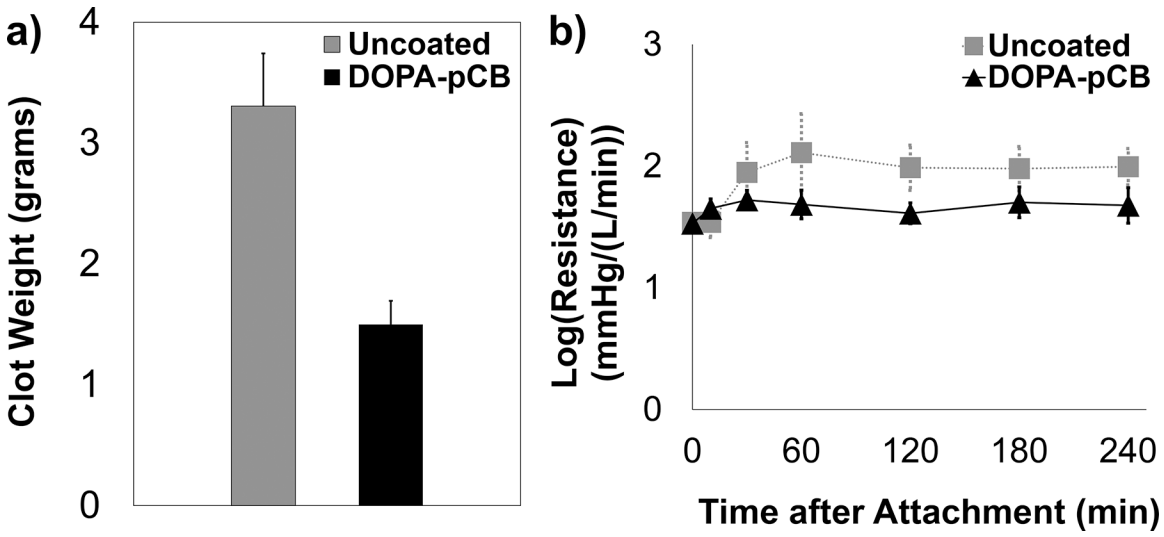

Figure 5:

Quantitative measurements of thrombus formation: a) total clot formation inside the micro artificial lung at end of the 4-hour rabbit study, $p < 0.05$, $N \geq 4$; b) log(Resistance) for micro-artificial lung in the 4-hour rabbit study, $N \geq 5$, $p = 0.18$. Error bars = S.E.M. for both figures

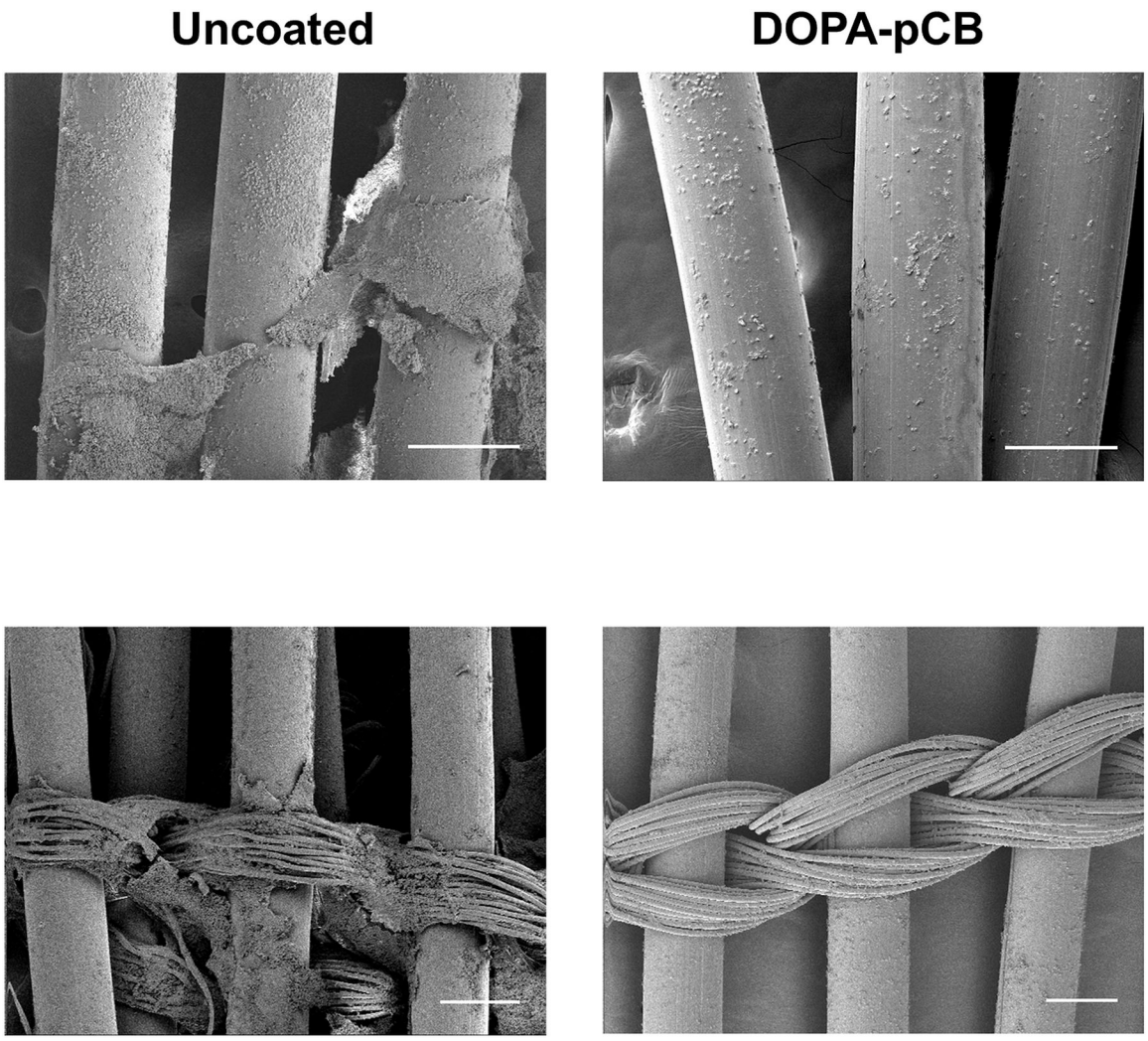

Figure 6:
Scanning electron microscope images of uncoated (left column) and DOPA-pCB (right column). Hollow fibers (top row) and finer weaving fibers (bottom row) are both shown. Scale bar = 200 μm for all four panels

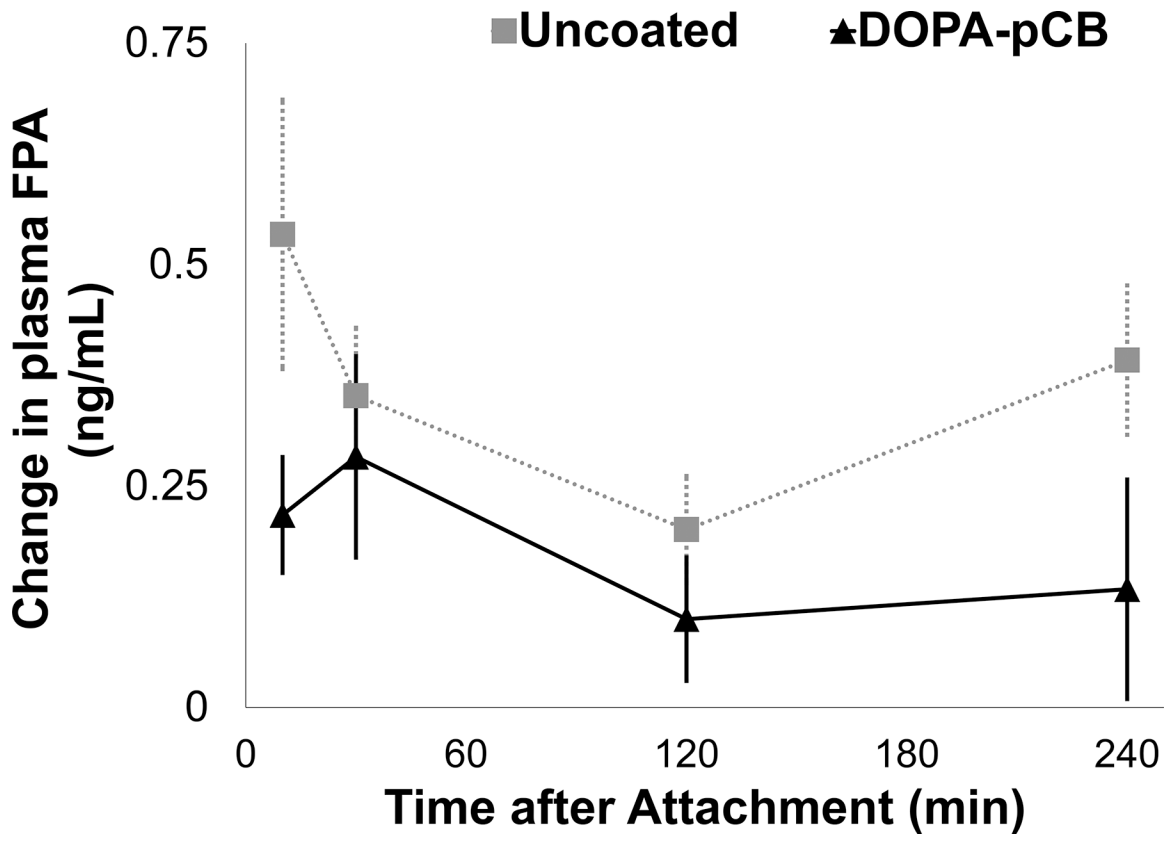

Figure 7:
The change in plasma fibrinopeptide A(FPA) level from baseline measurements, $p = 0.06$, $N \geq 5$, error bar = S.E.M.

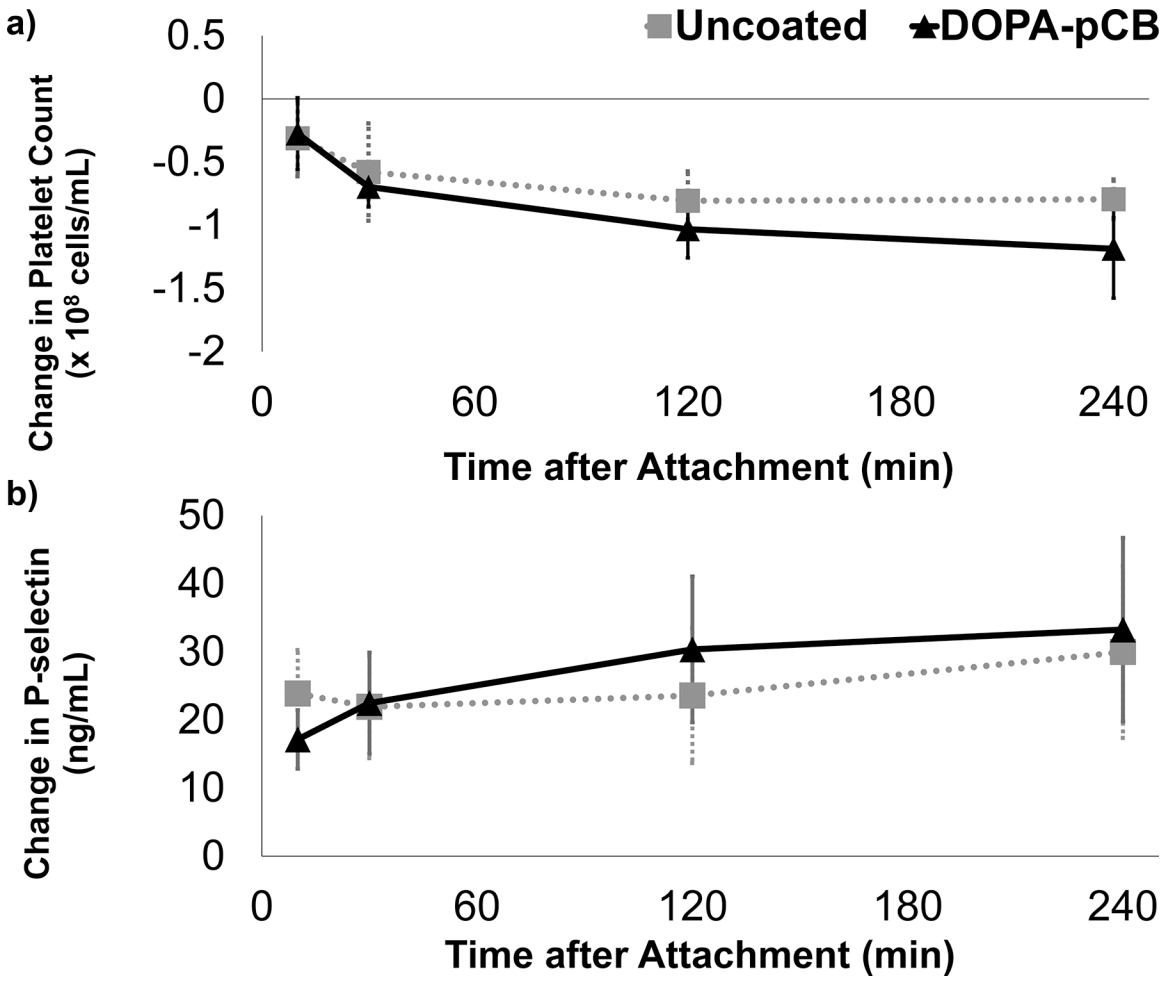

Figure 8:

Platelet activity and consumption during rabbit study: a) change in platelet count from baseline measurement, N ≥ 4; b) change in plasma p-selectin level from baseline measurement, N ≥ 4. Error bar = S.E.M. for both figures